Metrol. Meas. Syst., Vol. 29 (2022) No. 4, pp. 779–793
DOI: 10.24425/mms.2022.143070

PAN POLSKA AKADEMIA NAUK

METROLOGY AND MEASUREMENT SYSTEMS
Index 330930, ISSN 0860-8229
www.metrology.wat.edu.pl

M&MS

MACHINE VISION BASED VERNIER CALIPER READING TECHNOLOGY RESEARCH

Wen-Meng Chen, Hong-Xi Wang, Guan-Wei Wang, Wen-Hong Liang

Xi'an Technological University, School of Electrical and Mechanical Engineering, Xi'an, Shanxi 710021 China
(*chenwenmeng@st.xatu.edu.cn*, ✉ *whx_yz@163.com*, +86 137 0023 0315, *wangguanwei@xatu.edu.cn*, *xws-liangwenhong@163.com*)

Abstract

Accurate and fast access to Vernier caliper readings is a critical issue in automated verification of Vernier calipers. To address this problem, this paper proposes a machine vision-based algorithm for reading the Vernier caliper's displayed value. The suggested method first employs threshold segmentation and template matching to determine the region of interest and obtain the main ruler digit position by alternate projection. Then, we apply the improved LeNet5 network to identify the main ruler of the Vernier caliper, Moreover, we developed the first and last inscription method for reading the decimal part of the Vernier caliper and established our data set for model training. Extensive experiments on reading the displayed value have demonstrated our algorithm's accuracy, which achieves a displayed value reading accuracy of 100%. Compared to other methods, the proposed technique affords better stability and accuracy.

Keywords: Vernier calipers, convolutional neural networks, error averaging, alternate projection.

1. Introduction

As a precision gauge, Vernier calipers measure the length, inner diameter, outer diameter, and depth of various precision parts. Such instruments are widely used in the machinery manufacturing industry due to their ease of operation, high measurement accuracy, and low procurement cost, Nevertheless, the Vernier calipers suffer from manufacturing and assembly errors and wear, affecting their measurement accuracy and imposing unnecessary deviations in the measurement results. Therefore, calipers must be regularly calibrated to ensure their reliability. The Vernier caliper calibration process includes several tasks, such as appearance inspection, zero value error and indicating value error, involving 12 calibration tasks, of which the indicating value error calibration has the most extensive workload. Typically, a large manufacturing enterprise has 13,000 Vernier calipers in use and each must be checked per quarter. Given that the check is most often manual, the calibration process has low efficiency and is highly subjective. Therefore, automatic Vernier caliper calibration is necessary,

Article history: received April 12, 2022; revised July 26, 2022; accepted August 23, 2022; available online October 5, 2022.

One of the core technologies of automatic calibration is implementation of automatic reading of the Vernier caliper. Due to continuous rapid advance of both hardware and software technologies in camera and computing systems, Vision-Based Measurement had gained much research interest [1], as compared with the human eye, a camera can capture more information and process information in less time. For example, using machine vision to evaluate the metallic surfaces [2,3]. Xuebing *et al.* employed a camera to obtain a workpiece image, which they applied to realize precise measurements [4]. Yu *et al.* [5] developed a vision-based method to detect tool wear. With the development of deep learning, the CNN network has also entered the field of measurement, Researchers have explored various methods for pointer meter automatic recognition [6,7]. Zuo *et al.* proposed a deep learning-based automatic reading recognition method for pointer meters. This method has effectively solved the problems of uneven illumination in each image, complex backgrounds, tilting of pointer meters, image blur, and scale change. But in their experiments, each image has only on pointer [8]. Liu *et al.*, use a Faster Region-based Convolutional Network (Faster R-CNN) to detect the position of the target meter and obtain the reading by Hough Transform. Through the comprehensive application of feature correspondence and Perspective Transform, the problems of specular reflection and image distortion are solved to obtain high quality images [9]. Zhou *et al.* proposed a novel end-to-end intelligent reading method for a pointer meter based on deep learning, which locates the meter and extracts the pointer simultaneously without any prior information. This method has the advantage of being able to recognize pointer meters under complex conditions such as tilt, rotation, blur and illumination [10].

Moreover, realizing the indicator reading of a Vernier caliper through VBM technology has also been investigated. For instance. Bao *et al.* proposed an automatic reading device for Vernier calipers using a CCD camera to capture Vernier calipers imagery and performed digital recognition and reading of the indicated value through image filtering, binarization, and grayscale moment sub-pixel edge detection combined with the black and white mutation principle [11]. Wang *et al.*, designed a Vernier caliper automatic calibration device using a CMOS camera that captured Vernier caliper pictures and an alternate projection method to segment the numbers, a Hough transform scheme to detect the scale line and finally read the Vernier caliper indicated value [12], Although the two methods above suggest an automatic Vernier caliper reading device, their accuracy is poor. Thus. Ding *et al.* proposed an image recognition algorithm appropriate for digital display calipers based on the improved threading method. This work aimed to enhance the efficiency and recognition accuracy of digital caliper display recognition, but the method is limited to digital display calipers [13]. Yu *et al.* used the projection method to extract the main ruler digits and employed a convolutional neural network to recognize the extracted digits, Nevertheless, they did not propose a complete method to read the displayed value of Vernier calipers [14].

To address these shortcomings in the automated Vernier caliper reading technology, this paper proposes a machine vision-based Vernier caliper display value reading algorithm which exploits template matching to determine the rough position of the left and right zero positions of the Vernier caliper and define the region of interest for display value reading, Then, our method divides the main ruler and Vernier ruler through image binarization and uses the alternate projection method to extract the main ruler's digital picture. Finally, the developed method uses the improved LeNet5 network to identify the main scale of the Vernier caliper. Moreover, we suggest the first and last inscription method to read the decimal part of the Vernier caliper and detect the exact coordinates of the zero inscriptions before and after the Vernier caliper through a fitting method, which is used as the benchmark to deduce the coordinates of other inscriptions. This strategy avoids fitting to each scale line and thus reducing the time consumed to read the displayed value. Extensive experiments utilizing our data set built for model training demonstrate our algorithm's advantages over current methods in terms of accuracy and reading time.

Metrol. Meas. Syst., Vol. 29 (2022), No. 4, pp. 779–793
DOI: 10.24425/mms.2022.143070

The contributions of this paper are as follows:

1. Aiming at the universal Vernier caliper, a complete indicator reading method based on machine vision is proposed, and the LeNet5 network is used to recognize the number of the main ruler.
2. A new strategy is proposed to avoid detecting each scale when reading the decimal part of the Vernier caliper and to reduce the error caused by fitting the scale.
3. The test accuracy of the proposed method can reach 100%, which is better than other methods in existing articles.

The rest of this paper is organized as follows. Section 2 introduces the proposed method's general idea for the recognized Vernier caliper value, Then, this method is implemented and verified through experiments in Section 3. Finally, the conclusions and discussion are in Section 4.

2. Methods

Figure 1 illustrates the overall flow of the proposed algorithm. Once the Vernier caliper image is captured, the rough position of the front and rear zeroes of the Vernier scale are determined through the template matching method, defining the *Region of Interest* (ROI). Then, the image is pre-processed with tilt correction, filtering, and grayscaling, and the processed ROI image is segmented utilizing a threshold scheme to separate the main ruler from the Vernier ruler. The main ruler part is binarized and projected alternately to extract its digital part, and the latter is identified using an improved LeNet5 model. The fractional part of the main ruler is determined based on the Vernier zero scale to derive the main ruler display. The coordinates of the Vernier scale inscriptions are determined by the first and last inscription method, and the exact coordinates of the zero inscriptions first and last in the Vernier scale are determined by the fitting method, Additionally, the coordinates of the other inscriptions are deduced by this coordinate, and the coordinates of the primary scale inscriptions are detected utilizing the same method. Finally, the fractional part of the displayed value is determined by subtracting the coordinates of the main scale inscription and the Vernier scale inscription.

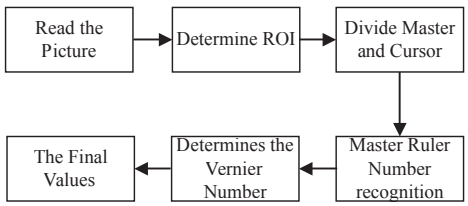

Fig. 1. System flowchart.

2.1. ROI area extraction

Once the camera acquires the Vernier caliper image, areas within the picture may be invalid for the Vernier caliper reading, and therefore the area containing the critical information needs to be filtered. During manual reading of the indicated value, the operator first finds the position of the left zero mark, and therefore our algorithm adopts the same method. Hence, we first manually capture the pictures of the Vernier scale's left and right zero positions and save them as templates. Based on the template matching method, we locate the rough positions of Vernier's left and right zero positions. The template matching method exploits the squared difference matching method [15], defined as:

$$R(x,y) = \sum_{x',y'} \left(T\left(x',y'\right) - I\left(x+x',y+y'\right)\right)^2. \tag{1}$$

Then, given the rough position of the left and right zero position as the boundary to extend outward to a certain length, we intercept the fixed ROI height that includes the Vernier caliper readings. An exemplary ROI region is illustrated in Fig. 2.

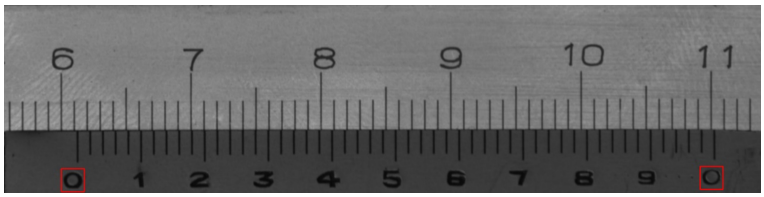

Fig. 2. ROI area.

2.2. Image pre-processing

During picture acquisition, the tilt phenomenon is evident. To facilitate the subsequent processing, the ROI region must be corrected for tilt employing the Hough line detection method to detect all lines in the ROI and calculate the mean tilt angle of all lines. From this process, we obtain the picture rotation angle θ:

$$\theta = \frac{1}{N}\sum_{i=1}^{N}\theta_i. \tag{2}$$

Fingerprints and various stains will be left on the caliper surface, while image noise will also affect the image quality. Therefore, we filter ROI to enhance the subsequent recognition process. Commonly used filtering functions are neighbourhood mean filtering, median filtering, Gaussian filtering, and bilateral filtering, with the corresponding filtering results illustrated in Fig. 3. The latter figure suggests that Gaussian filtering is more appropriate for the task examined in this paper, and therefore we employ Gaussian filtering to filter the ROI and eliminate noise.

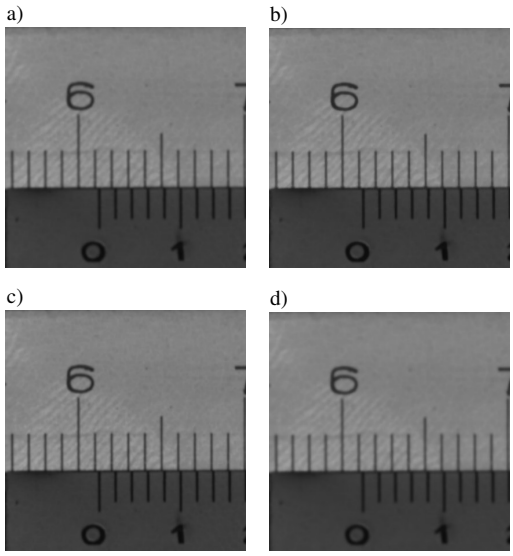

Fig. 3. (a) Mean Filtering, (b) Median Filtering, (c) Gaussian Filter, (d) Bilateral Filtering.

Metrol. Meas. Syst., Vol. 29 (2022), No. 4, pp. 779–793
DOI: 10.24425/mms.2022.143070

2.3. The main ruler and Vernier's separation

In the process of reading the master scale numbers, the ROI presents a noticeable gray difference between the Vernier and the master scale. The corresponding gray histogram of the ROI is depicted in Fig. 4a, highlighting a gray value distribution with a double-peak pattern, Therefore, we use the maximum inter-class variance method to perform threshold segmentation [16], with the corresponding results illustrated in Fig. 4b.

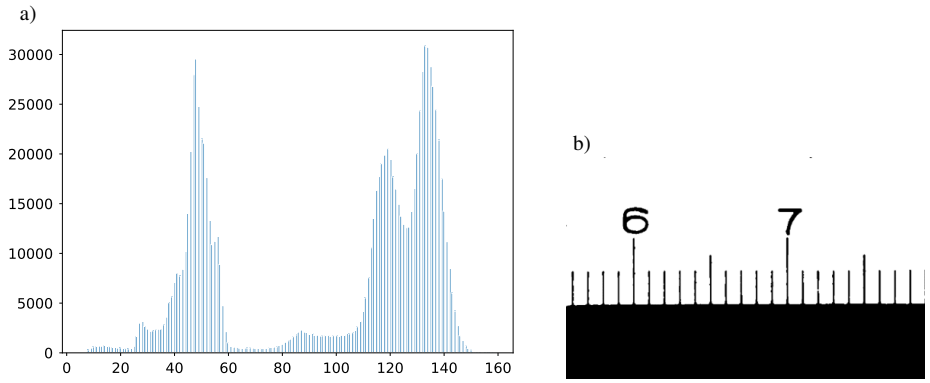

Fig. 4. (a) ROI gray histogram and (b) thresholded image.

The thresholded image presented above is projected horizontally to separate the main ruler area from the Vernier area (Fig. 5a). Then, these areas are separated by selecting an appropriate threshold (Fig. 5b and 5c).

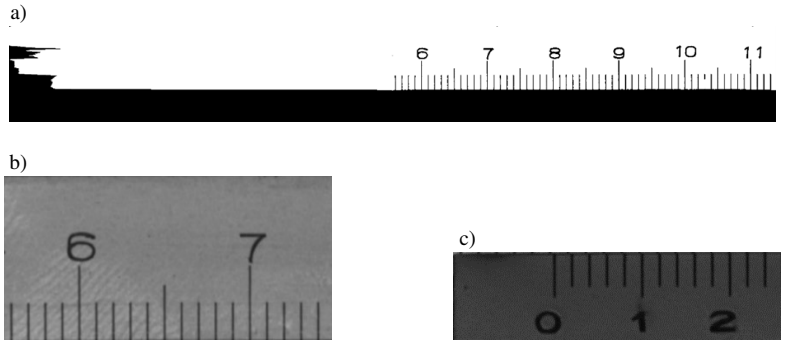

Fig. 5. (a) Horizontal projection of ROI area, (b) The main picture, (c) The cursor image.

2.4. Master ruler value read

2.4.1. Extract the master ruler number

Figure 6 is the flowchart of the reading method for the integer part of main ruler. In the section above, we obtained the main ruler image. In the reading process of the indicator value, we recognize a single digital image, Therefore, it is necessary to segment the overall digital image.

Firstly, we employ the maximum interclass variance method for the threshold segmentation process of the extracted master ruler images (Fig. 7). We perform horizontal projection on the thresholded images to separate the number part and the scales' part. Then we continue to project the number part vertically and break it (Fig. 8) into single number images. Finally, the distance from each image to the zero-scale position is calculated. With finding the minimum distance, the corresponding image is the number to be identified.

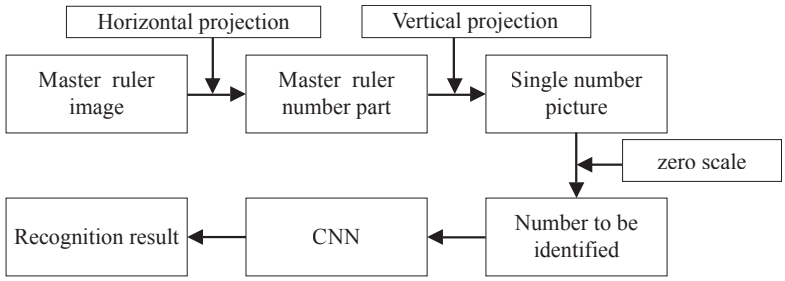

Fig. 6. Reading method of the integer part of the main ruler.

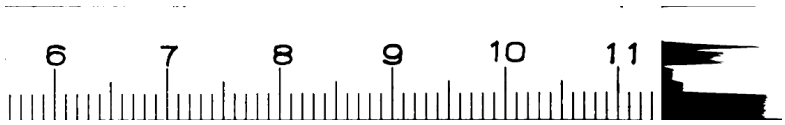

Fig. 7. Master ruler threshold image and horizontal projection.

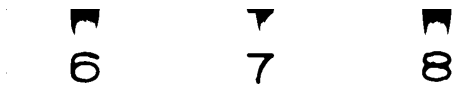

Fig. 8. Master ruler and digital segmentation projection results.

Long-term usage of a Vernier caliper creates surface scratches and stains that appear in the image interfering with the pixels containing valuable information and affecting the horizontal and vertical projection and, ultimately, the histogram-based thresholding process.

According to prior knowledge, if the width of the digital area of the Vernier caliper is W and the height is H, a certain proportion r_1, r_2 $(0 < r_1 r_2 < 1)$ can be set to eliminate the area with the projection width less than $r_1 W$ or the height less than $r_2 H$, to reduce the interference of stains and scratches on the caliper surface.

2.4.2. Master ruler digit recognition

Once the processing above is completed, we extract all the numbers contained in the ROI. Suppose the main ruler area contains N numbers and the abscissa of the center point of each number is x_i, $i = 1, 2, \ldots, N$. The cursor on the left side of the zero scale is the x_0 abscissa and while observing the ROI area, the zero scale on the right side will always have a number. Therefore, the algorithm recognizes the zero scale on the right side of the numbers and each number by calculating the center distance to the zero scale. Additionally, we select the zero scale

Metrol. Meas. Syst., Vol. 29 (2022), No. 4, pp. 779–793
DOI: 10.24425/mms.2022.143070

on the right side of the latest digit. Since the numbers are N, $N-1$ is the integer part of the master ruler.

Many scholars have proposed various algorithms for digital recognition [17–19]. Due to the rapid development of *convolutional neural networks* (CNNs), image recognition and classification based on CNNs have become increasingly mature. Therefore, this paper utilizes the classic LeNet5 [20] network and improves its adaptability by replacing average pooling with Maxpooling and employing the Linear Rectification Function (ReLU) [21] as the activation function. The proposed network structure is illustrated in Fig. 9. After each convolutional layer, the ReLU activation function forms a convolutional module combined with the maximum pooling layer. After two convolutional modules, the model is prevented from overfitting by using two fully connected layers and the Dropout technology [22, 23]. The specific network parameters are reported in Table 1.

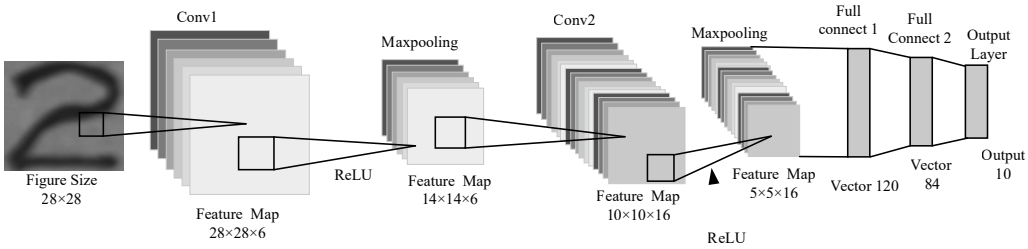

Fig. 9. LeNet5 structure.

Table 1. LeNet5 Parameters.

Network Structure	Kernel Size	Padding	Input	Output
Conv1	$5\times5\times6$	2	28×28	$28\times28\times6$
Maxpooling	$2\times2\times6$	0	$28\times28\times6$	$14\times14\times6$
Conv2	$5\times5\times16$	0	$14\times14\times6$	$10\times10\times16$
Maxpooling	$2\times2\times16$	0	$10\times10\times16$	$5\times5\times16$
Full Connect1	/	/	400	120
Full Connect2	/	/	120	84
Output Layer	/	/	84	10

Our network utilizes cross-entropy as the loss function, with the multi-classification cross-entropy loss function defined as follows:

$$L = \frac{1}{N}\sum L_i = -\frac{1}{N}\sum_{i}\sum_{c=1}^{M} y_{ic}\log\left(p_{ic}\right), \tag{3}$$

where M represents the number of categories, y_{ic} represents the label of sample I and p_{ic} represents the probability that sample I is correctly predicted. Compared with the *Mean Square Error Loss Function* (MSE), the cross entropy loss function has a larger gradient in the training process, and the model can converge faster.

We use the *Adaptive Moment Estimation* (Adam) [18] as the optimizer. Compared with the *Stochastic Gradient Descent* (SGD), Adam can dynamically adjust the fitting direction, accelerate

the model convergence and save training time. The Adam optimization update process is as follows:

$$g \leftarrow +\frac{1}{m}\nabla_\theta \sum_i L\left(f\left(x_i;\theta\right), y_i\right), \tag{4}$$

$$s \leftarrow \rho_1 s + (1-\rho_1)\, g, \tag{5}$$

$$\hat{s} \leftarrow \frac{s}{1-\rho_1}, \qquad \hat{r} \leftarrow \frac{r}{1-\rho_2}, \tag{6}$$

$$\triangle\,\theta = -\epsilon\frac{\hat{s}}{\sqrt{\hat{r}+\delta}}, \qquad \theta \leftarrow \theta + \triangle\,\theta, \tag{7}$$

where ϵ is the step value, θ is the initial parameter, δ is the numerical stability, ρ_1 is the first-order momentum attenuation coefficient, ρ_2 is the second-order momentum attenuation coefficient, s is the first-order momentum, r is the second-order momentum. From this process, we update s and r, and then calculate the parameter update according to s, r and the gradient.

2.5. Read the decimal part of the cursor caliper

Reading the decimal part of the Vernier caliper is the key to the entire Vernier caliper reading process. Hence, line detection on the Vernier caliper requires precision and stability, with current solutions involving fitting [12] and threading methods (black and white mutation) [11,24], Nevertheless, these methods require a clear binary image with less interference.

Given the problems above, this paper proposes the first and last inscription method to reduce the dependence on binary images and neglect the requirement to fit each scale. For example, we consider the Vernier caliper with a minimum dividing value of 0.02 mm and a measuring range of 200 mm. Manually reading the indicator numbers primarily depends on the distance between the main ruler and the Vernier line, as this distance is the judgment basis to find the nearest two lines, *i.e.*, the Vernier caliper decimal part.

This paper considers a minimum Vernier caliper degree value of 0.02 mm, producing 51 root grooves. Our method defines the rough groove position according to the one defined before and after the cursor zeroes. Then, the linear quasi zero scribed lines before and after are merged to obtain the accurate abscissa, *i.e.*, x_0 and x_{50}, where x_0 is the zero before the scribed line coordinates and x_{50} is the coordinate of the last zero notch line. The x-coordinate of the i-th notch line x_i $(i = 0, 1, 2, \ldots, 50)$ is:

$$x_i = \frac{x_{50} - x_0}{50} \times i. \tag{8}$$

According to the front and back zero lines of the Vernier, we find the nearest main ruler line to the left of x_0 and the nearest main ruler line to the right of x_{50}, respectively. We use the same method to calculate the abscissa of the main ruler line, and finally, we subtract the coordinates of the two-line groups.

In Fig. 10, the red and green lines are the detection results of the Vernier line and the primary ruler line, and the number is the distance difference between the upper and lower lines. The test results schematic diagram is illustrated in Fig. 11. The calculated result is saved in the matrix distance, and the red rectangular box mark is the minimum distance between the upper and lower lines.

According to the distance rule of the primary ruler and the Vernier scale, the elements in the matrix show a decreasing trend from positive to negative. According to this rule, the *index* before

Metrol. Meas. Syst., Vol. 29 (2022), No. 4, pp. 779–793
DOI: 10.24425/mms.2022.143070

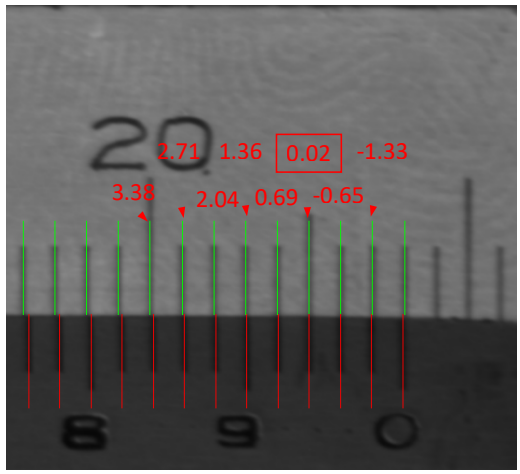

Fig. 10. Main ruler and Vernier scoring test results.

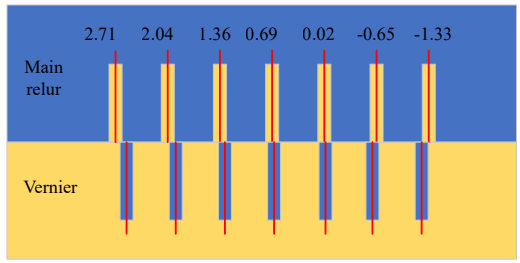

Fig. 11. Test results schematic diagram.

the negative element is taken from the distance matrix, namely, the number of the aligned Vernier scale lines. The num_{ver} of the Vernier scale is illustrated as follows:

$$num_{\text{ver}} = index \times 0.02. \tag{9}$$

3. Experiment and data analysis

3.1. Laboratory equipment

Based on the above caliper reading process, we designed an experimental device illustrated in Fig. 12. A Vernier caliper with a measuring range of 200 mm is taken as the experimental object. We used an MV-E2900M/C-M plane array camera and BT-R35F192 telecentric lens for the experiments. The parameters of the primary camera and lens are presented in Table 2. For completeness, it should be mentioned that the proposed algorithm was implemented in Python utilizing the OpenCV toolkit.

Good verticality between the camera's axis and Vernier caliper can keep the numbers at the left and right ends in the Vernier caliper image equal in size and thus we took some measures to make sure they were perpendicular. The lens used in the experiment is installed vertically on

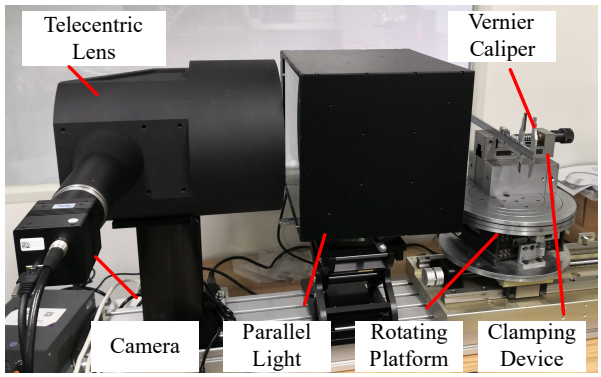

Fig. 12. Equipment used for experiments.

Table 2. Camera and lens parameters.

Camera Parameters	MV-E2900M/C-M	Lens Parameters	BT-R35F192
Highest Resolution	6576 × 4384	Magnification	0.187
Pixel Size	5.5 µm × 5.5 µm	Aperture	16
Maximum frame rate	2.5 fps	Working distance	400 ± 3% (mm)
Number of data bits	8	Depth of field	20 (mm)

the base, and the rotating platform is installed under the clamping device. First of all, the Vernier caliper is clamped, and then the rotating platform is gradually rotated by measuring the distance between the two sections (A. B in Fig. 13) of the Vernier caliper so that the Vernier caliper is perpendicular to the lens optical axis. The telecentric lens used in the experiment has a working distance of 400 mm and a depth of field 20 mm, which can ensure that the numbers at the left and right end of the image are the same.

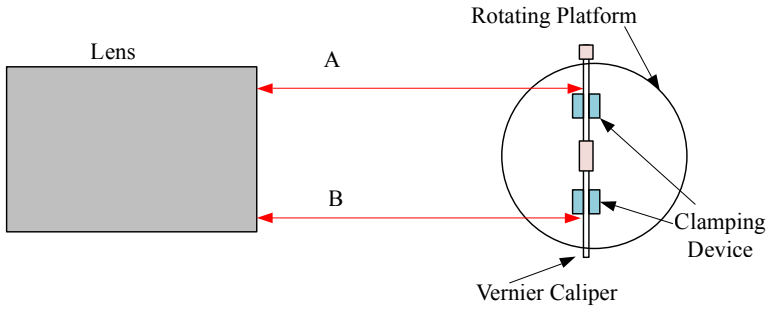

Fig. 13. Sketch diagram of parallelism adjustment.

3.2. Experimental results of digital recognition

The LeNet5 network is specially used to recognize handwritten digits. LeNet5 is trained on the MNIST handwritten data set, including 60,000 training and 10,000 testing images. In this work, we train our network on the MNIST data set for 20 epochs. MINST handwritten numbers are

Metrol. Meas. Syst., Vol. 29 (2022), No. 4, pp. 779–793
DOI: 10.24425/mms.2022.143070

slightly different from the printed numbers used by Vernier calipers, and the numerical recognition effect of the model after training is not ideal for Vernier calipers, Therefore, it is necessary to learn the character characteristics of Vernier calipers while still exploiting the MNIST data set. Hence, to improve the recognition accuracy, 1340 digital character images of Vernier calipers were collected to train the model. After pre-processing, these images were saved as single-channel images of size 28×28 pixels and were labeled accordingly. The final data were saved in CSV files for later use. The collected data set is depicted in Fig. 14a.

The model was re-trained on our data set, involving a random confusion strategy during loading the dataset. From the 1340 digital character images, 1000 were randomly selected for training and 340 for testing. The training and test results are illustrated in Fig. 14b.

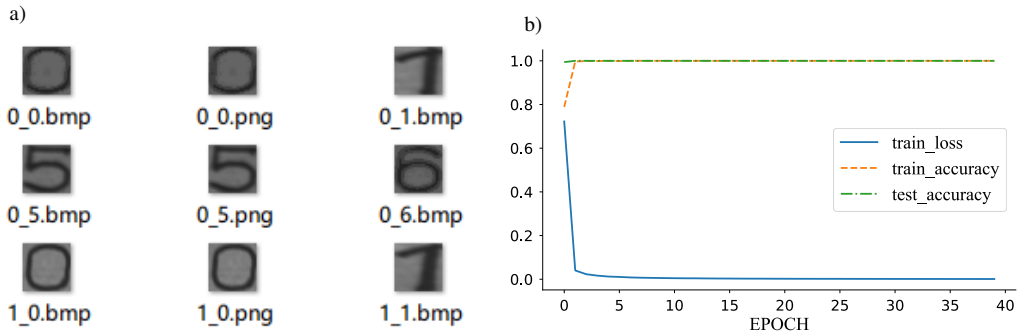

Fig. 14. (a) Vernier number data set. (b) Training and testing results on our dataset.

Our model was trained for 40 epochs, while after each epoch we evaluated the trained model on the test set. After 40 training rounds, the model's recognition accuracy reached 100% on the test set, meeting the requirements of number recognition in the verification process.

3.3. Vernier caliper shows value decimal reading experiment

The detection results of the first and last inscription method proposed in this paper are depicted in Fig. 14. The latter figure highlights that the cutting line detection of the main ruler and the Vernier is complete and accurate. To further verify the feasibility of the first and last inscription method, we challenge it in 40 experiments against the threading method [11] and the fitting method [12]. The corresponding errors of both methods are illustrated in Fig. 15, indicating a

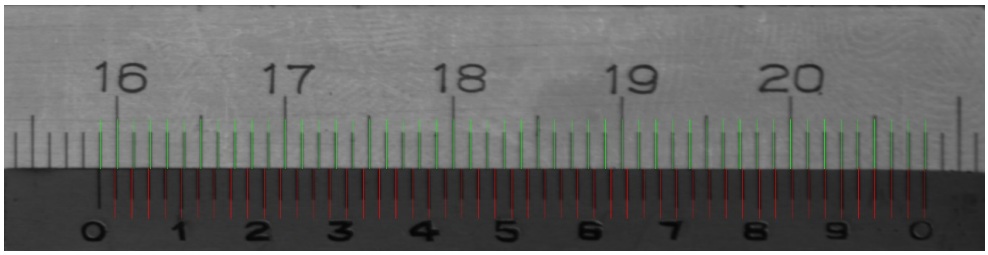

Fig. 15. The results of the head and tail engraving method.

value error in 7 of the 40 experiments for the threading method, 4 of the 40 experiments for the fitting method and no value error in all 40 experiments for the first and last inscription method. Therefore, we have demonstrated that the first and last inscription method is the more accurate in detecting cutting lines, it only needs to fit the two head-to-tail cutting lines, and the processing speed is bigger than in the case of the fitting method.

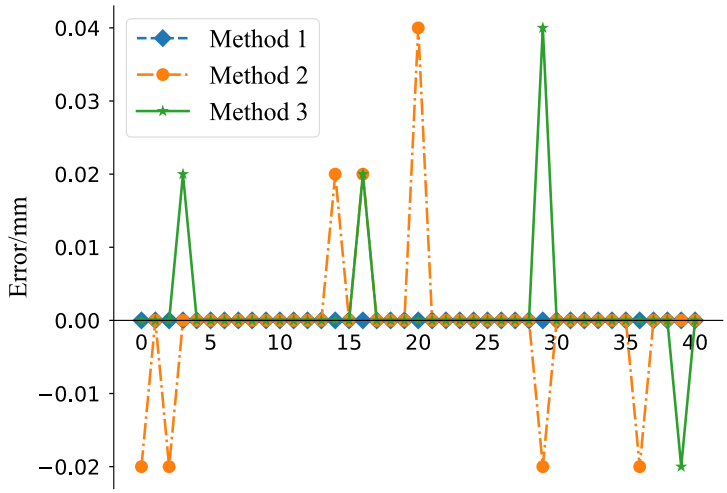

Fig. 16. Comparison of head-to-tail scale method (Method 1), threading method (Method 2) and fitting method (Method 3).

3.4. Identification results of the whole system

We challenged the proposed method in 10 experiments against the method 1 [11] and the method 2 [12]. Our method achieves the highest accuracy. Method 1 has value errors of 2 in 10 experiments, with an accuracy of 80%, and Method 2 has a value error of 1 in 10 experiments, with an accuracy of 90%.

Table 3. Comparative experiment between the proposed method and other methods.

Number	1	2	3	4	5	6	7	8	9	10	**Accuracy**
Manual reading	0.04	5.66	7.24	11.24	16.28	23.12	61.24	125.14	150.48	159.00	–
Our Method	0.04	5.66	7.24	11.24	16.28	23.12	61.24	125.14	150.48	159.00	100%
Method 1	0.04	5.66	7.24	11.26	16.28	23.12	61.24	125.14	150.50	159.00	80%
Method 2	0.04	5.64	7.24	11.26	16.28	23.12	61.24	125.14	150.50	159.00	90%

We performed 48 display value reading tests utilizing the proposed algorithm, requiring 170.88s and an average time of 3.56s per image. The test results are reported in Table 4, and are compared against the manual readings revealing a 100% reading accuracy.

Metrol. Meas. Syst., Vol. 29 (2022), No. 4, pp. 779–793
DOI: 10.24425/mms.2022.143070

Table 4. Algorithm test results.

Number	Manual Reading (mm)	Algorithm Reading (mm)	Number	Manual Reading (mm)	Algorithm Reading (mm)	Number	Manual Reading (mm)	Algorithm Reading (mm)
1	0.02	0.02	*17*	14.78	14.78	*33*	61.24	61.24
2	0.04	0.04	*18*	16.00	16.00	*34*	79.12	79.12
3	3.44	3.44	*19*	16.28	16.28	*35*	81.14	81.14
4	3.46	3.46	*20*	17.54	17.54	*36*	92.54	92.54
5	5.66	5.66	*21*	18.96	18.96	*37*	111.52	111.52
6	6.64	6.64	*22*	19.48	19.48	*38*	119.42	119.42
7	7.24	7.24	*23*	20.02	20.02	*39*	125.14	125.14
8	9.00	9.00	*24*	21.7	21.70	*40*	130.84	130.84
9	10.48	10.48	*25*	22.00	22.00	*41*	150.48	105.48
10	10.56	10.56	*26*	23.12	23.12	*42*	156.86	156.86
11	10.90	10.90	*27*	24.08	24.08	*43*	156.86	156.86
12	11.24	11.24	*28*	24.82	24.82	*44*	156.88	156.88
13	11.30	11.30	*29*	33.16	33.16	*45*	159.00	159.00
14	11.36	11.34	*30*	33.86	33.86	*46*	173.48	173.48
15	12.94	12.94	*31*	36.00	36.00	*47*	191.78	191.78
16	13.44	13.44	*32*	43.30	43.30	*48*	198.86	198.86

4. Conclusions

Automatic reading of the Vernier caliper value is essential in automatic caliper verification. In the proposed automatic Vernier caliper value reading method, we employ template matching to extract the ROI, obtain the numbers on the calipers by alternate projection, and improve the LeNet5 network to recognize the caliper numbers. To read the decimal part of the Vernier caliper, this paper suggests the application of the first and last inscription method which mainly detects the beginning and ending zero scale line, calculates the middle scale line coordinate utilizing the coordinates of the beginning and ending zero scale line, and compares the reading result by showing the value based on the threading method. Extensive experiments demonstrate a 100% accuracy on 48 reading experiments with an average processing time of 3.56 s per image.

Our method's shortcoming is that the alternate projection is inefficient, and therefore future work will explore the method of direct positioning the Vernier calipers.

Acknowledgements

This work was supported by the Department of Science and Technology of Shaanxi Province. China (grant # 2020ZDLGY14-02, grant # 2019zdzx01-02-02).

The authors would like to express their gratitude to EditSprings (https://www.editsprings.cn) for the expert linguistic services provided.

References

[1] Shirmohammadi, S., & Ferrero. A. (2014). Camera as the instrument: the rising trend of vision based measurement. *IEEE Instrumentation Measurement Magazine*, *17*(3), 41–47. https://doi.org/10.1109/MIM.2014.6825388

[2] Borwankar, R., & Ludwig, R. (2020). A novel compact convolutional neural network for real-time non-destructive evaluation of metallic surfaces. *IEEE Transactions on Instrumentation and Measurement*, *69*(10), 8466–8473. https://doi.org/10.1109/TIM.2020.2990541

[3] Liu, Y., Gao, H., Guo, L., Qin. A.. Cai. C., & You, Z. (2019). A data-flow oriented deep ensemble learning method for real-time surface defect inspection. *IEEE Transactions on Instrumentation and Measurement*, *69*(7), 4681–4691. https://doi.org/10.1109/TIM.2019.2957849

[4] Li, X., Yang, Y., Ye, Y., Ma, S., & Hu. T. (2021). An online visual measurement method for workpiece dimension based on deep learning. *Measurement*, *185*, 110032. https://doi.org/10.1016/j.measurement.2021.110032

[5] Yu. J.. Cheng, X., Lu, L., & Wu. B. (2021). A machine vision method for measurement of machining tool wear. *Measurement*, *182*, 109683. https://doi.org/10.1016/j.measurement.2021.109683

[6] Yang, Y., Wu, H., Wang, P., & Yang. F. (2020). Substation pointer meters detection and reading based on CNN. *International Symposium on Artificial Intelligence and Robotics 2020*. https://doi.org/10.1117/12.2575960

[7] Zhang, X.. Dang, X., Lv, Q., & Liu, S. (2020. April). A pointer meter recognition algorithm based on deep learning. In *2020 3rd International Conference on Advanced Electronic Materials. Computers and Software Engineering (AEMCSE)* (pp, 283–287). IEEE. https://doi.org/10.1109/AEMCSE50948.2020.00068

[8] Zuo, L., He, P., Zhang. C., & Zhang, Z. (2020). A robust approach to reading recognition of pointer meters based on improved mask-RCNN. *Neurocomputing*, *388*, 90-101. https://doi.org/10.1016/j.neucom.2020.01.032

[9] Liu, Y., Liu. J., & Ke, Y. (2020). A detection and recognition system of pointer meters in substations based on computer vision. *Measurement*, *152*, 107333. https://doi.org/10.1016/j.measurement.2019.107333

[10] Zhou. D., Yang, Y., Zhu. J., & Wang, K. (2022). Intelligent reading recognition method of a pointer meter based on deep learning in a real environment. *Measurement Science and Technology*, *33*(3), 055021. https://doi.org/10.1088/1361-6501/ac4079

[11] Chengde. B., Zhiling, X., Pengfeng, W., Wangda. C., & Lei, Y. (2016). Design of a device for the indication verification of Vernier calipers. *Journal of China University of Metrology, 27*(02), 138–143. https://doi.org/10.3969/j.issn.1004-1540.2016.02.003 (in Chinese)

[12] Mengpei, W., & Houyun, Y. (2019). Research on Automatic Verification Method of Vernier Caliper Indication Error. *Machine Building & Automation*, *49*(6), 203–205. https://doi.org/10.19344/j.cnki.issn1671-5276.2020.06.053 (in Chinese)

[13] Shuang. D., Guo-ying, R.. Fu-min, Z., & Nai-yin, F. (2019). Improved Threading Method for Caliper Image Recognition, *40*(3), 765–769. https://doi.org/10.3969/j.issn.1000-1158.2019.05.04 (in Chinese)

[14] Houyun, Y., Huiqing, W., Wei, W., & Yue, J. (2020). Identification of Numbers for Vernier Caliper Automatic Verfication System Based on Convolution Neural Network. *Chinese Journal of Sensors and Actuators*, *33*(12), 1718–1726. https://doi.org/10.3969/j.issn.1004-1699.2020.12.007 (in Chinese)

[15] Hashemi, N. S.. Aghdam, R. B., Ghiasi. A. S. B., & Fatemi, P. (2016). Template matching advances and applications in image analysis. *arXiv preprint arXiv:1610.07231*. https://doi.org/10.48550/arXiv.1610.07231

Metrol. Meas. Syst., Vol. 29 (2022), No. 4, pp. 779–793
DOI: 10.24425/mms.2022.143070

[16] Otsu, N. (1979). A Threshold Selection Method from Gray-Level Histograms. *IEEE Transactions on Systems Man & Cybernetics*, *9*(1), 62–66. https://doi.org/10.1109/TSMC.1979.4310076

[17] Yi-yan, S.. Dong-lin. T., Xu-long, W., Li, Z., & Bei-xuan, Q. (2021). Study on Digital Tube Image Reading Combining Improved Threading Method with HOG+SVM Method. *Computer Science*, *48*(11A), 396–399. https://doi.org/10.11896/jsjkx.210100123

[18] Ahlawat, S.. Choudhary. A., Nayyar. A., Singh, S., & Yoon. B. (2020). Improved Handwritten Digit Recognition Using Convolutional Neural Networks (CNN). *Sensors*, *20*(12), 3344. https://doi.org/10.3390/s20123344

[19] Salemdeeb, M., & Erturk, S. (2021). Full depth CNN classifier for handwritten and license plate characters recognition. *Peerj Computer Science*, *7*, e576. https://doi.org/10.7717/peerj-cs.576

[20] Lecun, Y., & Bottou, L. (1998). Gradient-based learning applied to document recognition. *Proceedings of the IEEE*, *86*(11), 2278–2324. https://doi.org/10.1109/5.726791

[21] Ide, H., & Kurita. T. (2017, May). Improvement of learning for CNN with ReLU activation by sparse regularization. In *2017 International Joint Conference on Neural Networks (IJCNN)* (pp. 2684–2691). IEEE. https://doi.org/10.1109/IJCNN.2017.7966185

[22] Hinton, G. E., Srivastava, N., Krizhevsky. A., Sutskever, I., & Salakhutdinov, R, R. (2012). Improving neural networks by preventing co-adaptation of feature detectors, arXiv preprint arXiv:1207.0580. https://doi.org/10.48550/arXiv.1207.0580

[23] Srivastava, N., Hinton, G., Krizhevsky. A., Sutskever, I., & Salakhutdinov, R. (2014). Dropout: A Simple Way to Prevent Neural Networks from Overfitting. *Journal of Machine Learning Research*, *15*(1), 1929–1958. https://jmlr.org/papers/volume15/srivastava14a/srivastava14a.pdf

[24] Wangda. C., Zhiling, X., & Zhifei, L. (2019). Design of Indication Verification Device for External Diameter Micrometer Based on Machine Vision. *Machine Tool & Hydraulics*, *47*(17), 115–119. https://doi.org/10.3969/j.issn.1001-3881.2019.17.021 (in Chinese)

Wenmeng Chen received the B.Sc, degree from Henan Normal University. China, in 2016 and received the M.Sc, degree from Guilin University of Electronic Technology. China, in 2020. Currently, he is a doctoral student atf Xi'an Technological University, His current research interests include precision measurement theory and instrument, deep learning and version measurement.

Guanwei Wang received the Ph.D, degree from Xi'an Jiaotong University. China, in 2013, He is currently a Lecturer at the School of Mechanic Engineering of Xi'an Technological University, His research activity focuses on mechatronic information systems, signal processing, machine vision, pattern recognition, etc.

Hongxi Wang received the Ph.D, degree from Xidian University, China, in 2006, He is currently a Full Professor and Dean of the School of Mechanic Engineering of Xi'an Technological University, His research activity focuses on precision measurement theory and instrument design, compliant mechanisms and intelligent sensors.

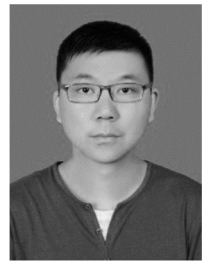

Wenhong Liang received the B.Sc, degree in mechanical and electronic engineering, the M.S degree in mechanical design and theory and the Ph.D, degree in mechanical engineering from Xi'an University of Technology. China, in 1999, 2007 and 2014, respectively. At present, he is a lecturer at Xi'an University of Technology, focusing on the detection and online status analysis of high-precision parts and equipment.